

Calculation of the Vibrational Spectra of H_5O_2^+ and Its Deuterium-Substituted Isotopologues by Molecular Dynamics Simulations[†]

Martina Kaledin*

Department of Chemistry and Biochemistry, Kennesaw State University, Kennesaw, Georgia 30144

Alexey L. Kaledin and Joel M. Bowman

Department of Chemistry, Emory University, Atlanta, Georgia 30322

Jing Ding and Kenneth D. Jordan

Department of Chemistry, University of Pittsburgh, Pittsburgh, Pennsylvania 15260

Received: January 25, 2009; Revised Manuscript Received: March 17, 2009

In this work, we present infrared spectra of H_5O_2^+ and its D_5O_2^+ , D_4HO_2^+ , and DH_4O_2^+ isotopologues calculated by classical molecular dynamics simulations on an accurate potential energy surface generated from CCSD(T) calculations, as well as on the BLYP DFT potential energy surface sampled by means of the Car–Parrinello algorithm. The calculated spectra obtained with internal energies corresponding to a temperature of about 30 K are in overall good agreement with those from experimental measurements and from quantum dynamical simulations.

I. Introduction

Protons (H^+) and hydroxide ions (OH^-) exhibit anomalously high mobility in aqueous media compared to other ions such as sodium (Na^+) and chlorine (Cl^-),¹ indicating that their transport occurs via mechanisms other than simple ionic diffusion. The nature of the excess proton and its transport mechanism and spectroscopic signatures in aqueous solutions have been the subject of extensive debate for many years.^{2–4} Much of this discussion has centered around H_3O^+ and H_5O_2^+ that are the ion cores of the so-called Eigen⁵ and Zundel⁶ forms of the cations, respectively. The Eigen designation is generally reserved for the H_9O_4^+ entity with the H_3O^+ hydronium core. Fluctuations between these species mediate the Grotthuss mechanism⁷ for proton transport.

Over the past few years, vibrational spectra have been obtained for mass-selected inert gas atom tagged $\text{H}^+(\text{H}_2\text{O})_n$ ions with n ranging from 2 to 8.^{8–15} These spectra have provided evidence for both Zundel and Eigen ions, as well as for species whose spectra are intermediate between those of Eigen and Zundel ions.¹³ Particularly noteworthy is the appearance of a doublet in the region ($\sim 1000\text{ cm}^{-1}$) of the shared proton stretch in the measured vibrational predissociation spectra of the $\text{H}_5\text{O}_2^+\text{Ne}$ and $\text{H}_5\text{O}_2^+\text{Ar}$ Zundel ions.¹⁴ This doublet has proven especially challenging theoretically,^{14,16} and it was first successfully characterized theoretically by Meyer and co-workers^{17,18} using the multiconfigurational time-dependent Hartree (MCTDH) method¹⁹ and accurate ab initio potential energy and dipole moment surfaces from Bowman and co-workers.²⁰ These calculations revealed that the doublet arises from a resonance between the shared proton O–H–O stretch and a combination state involving one quantum of the O–O stretch and two quanta of the water wag.

Unfortunately, it is difficult to apply the MCTDH method to larger protonated clusters due to the prohibitive computational costs of generating accurate potential energy surfaces from ab initio calculations and of doing the quantum dynamics calculations. As a result, there is considerable interest in establishing the applicability of more approximate methods for calculating the vibrational spectra of $\text{H}^+(\text{H}_2\text{O})_n$ clusters and other highly anharmonic species. This leads naturally to the question as to whether spectra calculated from the dipole autocorrelation function evaluated using “ab initio molecular dynamics” (AIMD) simulations can recover the key spectral features of such challenging systems. In the AIMD approach the energies, forces, and dipole moment functions for the sampled configurations are calculated “on the fly” using electronic structure methods. This approach has been used in several prior studies to obtain the vibrational spectrum of H_5O_2^+ .^{16,21–23} However, with one exception, these simulations were performed at internal energies, corresponding to temperatures of 80 K or higher, which are likely much higher than those of the Ne or Ar atom tagged clusters studied experimentally. The calculated spectrum reported in ref 23 does not provide clear-cut evidence of the doublet in the region of the shared proton asymmetric stretch, while that reported in ref 21, calculated at an internal energy content corresponding to $T = 300\text{ K}$, displayed considerable structure in this region. In a recent paper, Kim and co-workers reported the results of AIMD simulations of H_5O_2^+ carried out at an internal energy corresponding to $T = 50\text{ K}$.²² The resulting IR spectrum does display a doublet in the vicinity of the shared proton. It should also be noted that MD simulations carried out at an internal energy corresponding to $T = 100\text{ K}$ on an ab initio CCSD(T) potential energy surface²⁰ do display a doublet in the shared proton stretch region.¹⁶

In the present study, we report vibrational spectra of H_5O_2^+ and several of its D-substituted isotopologues, calculated using AIMD simulations as well as using MD simulations on the CCSD(T) potential energy and MP2-level dipole moment

[†] Part of the “Robert Benny Gerber Festschrift”.

* To whom correspondence should be addressed. Fax: +1-770-423-6744. E-mail: mkaledin@kennesaw.edu.

surfaces of Bowman and co-workers.²⁰ Internal energies corresponding to temperatures as low as 30 K are considered. It is demonstrated that for $T = 30$ K both sets of classical simulations give vibrational spectra, including the shared proton stretch region, in overall good agreement with experiment.

II. Computational Details

The AIMD simulations were carried out using the Car–Parrinello (CPMD) algorithm,^{24,25} together with the BLYP density functional method,^{26,27} the norm-conserving Troullier–Martins pseudopotential,²⁸ and a plane-wave cutoff of 120 Ry. Cluster boundary conditions were applied using the method of Martyna and Tuckerman.²⁹ A time step of 3 au (~ 0.073 fs) and a fictitious electron mass of 400 au were employed. The production runs were carried out for 170 000 steps in the microcanonical ensemble, following 30 000 step equilibration periods using the Nosé–Hoover thermostat.^{30–32} Rotational corrections³³ were applied every 20 steps. The first 20 000 steps of the microcanonical trajectories were discarded, and the remaining steps were used to compute average temperatures and spectra. The CPMD simulations on H_5O_2^+ were carried out for internal energy contents corresponding to temperatures ranging from 1 to 200 K, while those for the various D-substituted isotopologues were carried out only for internal energies corresponding to $T = 30$ K. The $T = 1$ K simulations were carried out as a check on possible errors caused by the use of the 400 au fictitious electron mass.³⁴ The IR absorption spectra were calculated from the Fourier transform of the dipole–dipole time correlation function, applying the harmonic quantum correction factor^{35,36}

$$Q = \frac{\beta\hbar\omega}{1 - \exp[-\beta\hbar\omega]}$$

Due to the considerable computational effort required to perform the CPMD simulations, each reported spectrum was obtained by averaging over one long-time trajectory. The CPMD simulations were carried out using the CPMD program (version 3.11.1).³⁷

Given the importance of both diagonal and off-diagonal anharmonicities in the vibrational spectrum of H_5O_2^+ , it is not clear a priori whether the BLYP functional describes the potential energy surface (PES) sufficiently accurately to properly account for the Fermi resonances observed in the experimental vibrational spectrum. For this reason, MD simulations on H_5O_2^+ and its D-substituted isotopologues were also carried out using the CCSD(T) PES and MP2 dipole moment function of Bowman and co-workers.²⁰ In the ensuing discussion this approach will be referred to as MD/CCSD(T).

The MD/CCSD(T) simulations of H_5O_2^+ and its D-substituted isotopologues were carried out in the NVT ensemble with internal energies corresponding to $T = 30$ and 50 K. For each temperature, 100 separate MD simulations were run. The initial velocities were sampled from the usual thermal distribution. Metropolis sampling was employed to select the initial geometries. In this sampling 200 steps were sufficient to obtain the thermal distribution for the initial geometries, as reported in our previous paper.¹⁶ A total of 100 (real-time) trajectories with these initial conditions were carried out for 16 ps, employing a time step of 0.25 fs. To achieve convergence of the phase space integration with only 100 trajectories, the dipole correlation function from each trajectory was also time averaged over the length of the propagation as discussed in ref 16. The resulting spectra yield a 2 cm^{-1} resolution. Additional details of the calculation of the spectra for the MD/CCSD(T) procedure can be found in section 2.1 in ref 16. For comparative purposes,

TABLE 1: Harmonic Vibrational Frequencies (cm^{-1}) of H_5O_2^+ and Its D-Substituted Isotopologues^a

H_5O_2^+	D_5O_2^+	$\text{DH}_4\text{O}_2^+(\text{int})$	$\text{DH}_4\text{O}_2^+(\text{ext})$	$\text{D}_4\text{HO}_2^+(\text{int})$	$\text{D}_4\text{HO}_2^+(\text{ext})$
170	121	170	156	121	131
339	248	311	307	261	257
471	339	444	447	350	363
532	389	488	482	407	423
554	420	547	534	423	439
630	593	626	627	593	608
861	627	692	846	786	647
1494	1084	1173	1449	1219	1104
1574	1145	1244	1487	1303	1158
1720	1257	1675	1663	1522	1280
1770	1298	1707	1740	1584	1508
3744	2694	3743	2753	2695	2699
3750	2703	3750	3747	2703	2752
3832	2811	3832	3794	2811	2811
3832	2811	3832	3832	2812	3793

^a Computed using the CCSD(T)-determined potential energy surface of ref 20.

the vibrational frequencies of H_5O_2^+ and its D-substituted isotopologues (Table 1) and intensities were also calculated in the harmonic approximation using the potential energy and dipole moment surfaces of Bowman and co-workers.²⁰

III. Results and Discussion

A. Effects of Temperature on the Calculated Spectra.

Before presenting the results of this subsection, it is worth noting some fundamental differences between classical and quantum calculations of spectra. At $T = 0$ K the former reproduce harmonic spectra in both line positions and intensities, whereas exact quantum spectra can (and generally do) display significant deviations from harmonic spectra due to diagonal and coupled anharmonic effects. As the temperature increases classical spectra also differ from harmonic spectra due to the classical response to anharmonic effects. In general, the expectation is that classical and quantum spectra do not describe these anharmonic effects equivalently; however, the dearth of comparisons between exact quantum and classical spectra at nonzero temperatures precludes making quantitative statements about their differences. Thus, when comparing classical, quantum, and experimental spectra, especially at low temperatures, it is important to keep this in mind.

Figure 1 reports the IR spectra of H_5O_2^+ calculated using the CPMD method for temperatures ranging from 1 to 200 K. The energy scale for these spectra has been multiplied by 1.029, which brings the energies of the calculated peaks in the $T = 1$ K spectrum into close agreement with the harmonic spectrum calculated using the Hessian and the same electronic structure method. This scaling approximately compensates for the unphysical red shifts caused by the use of a 400 au effective electron mass and is applied to all CPMD spectra reported in this paper. In contrast to the spectrum calculated for $T = 1$ K, that calculated for $T = 30$ K gives a pair of lines of comparable intensity near 1000 cm^{-1} , with a splitting of about 100 cm^{-1} , in close agreement with the experimental predissociation spectrum of $\text{H}_5\text{O}_2^+\text{Ne}$,¹⁴ which is reproduced in Figure 3. At $T = 50$ K the doublet in the calculated spectrum is still discernible although the lower energy feature has an intensity less than 1/10 that of the higher energy feature. As the temperature is increased further, the doublet structure disappears, and the calculated spectrum evolves into a broad structure spanning about 200 cm^{-1} . Although the temperatures of the clusters characterized experimentally are not known, it is clear that the Ne tagged cluster must be very cold, otherwise the Ne atom would be lost

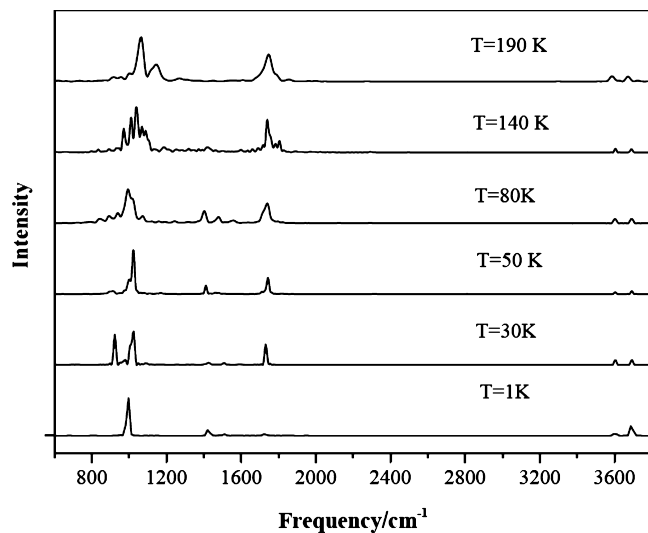


Figure 1. CPMD IR spectra of H_5O_2^+ for temperatures ranging from 1 to 200 K.

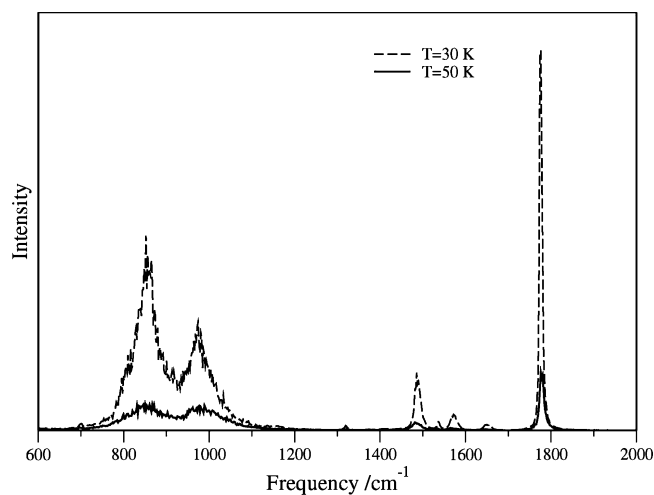


Figure 2. Temperature dependence of the MD/CCSD(T) IR spectrum for H_5O_2^+ , $T = 30$ K (dashed line), $T = 50$ K (solid line).

prior to photon absorption. With the caveats of the first paragraph of this subsection in mind, the results presented in Figure 1 suggest that the temperature of the Ne tagged H_5O_2^+ cluster is near 30 K, a conclusion also recently reached by McCoy and co-workers (for the Ar atom tagged cluster).³⁸ These results suggest that the failure of previous AIMD simulations to provide clear-cut evidence for a doublet near 1000 cm^{-1} is a consequence of the much higher temperatures employed.

Figure 2 displays the IR spectra of H_5O_2^+ calculated from MD/CCSD(T) simulations at $T = 30$ and 50 K. Overall, the resulting spectra are in close agreement with those obtained at the same temperatures using the CPMD method with the BLYP functional. The main difference between the spectra calculated using the two MD approaches is that in the MD/CCSD(T) simulations the doublet near 1000 cm^{-1} occurs about 70 cm^{-1} more to the red and, thus, in poorer agreement with experiment. However, it should be noted that the harmonic frequency for the shared proton stretch is about 100 cm^{-1} lower for the CCSD(T) PES than for the BLYP PES (861 vs 982 cm^{-1} , respectively) and that anharmonic corrections increase the shared proton stretch frequency by over 100 cm^{-1} .²¹ Thus, it appears that the better agreement with experiment of the frequencies in the shared proton stretch region of the spectrum calculated using the CPMD method is fortuitous, being the result of the DFT

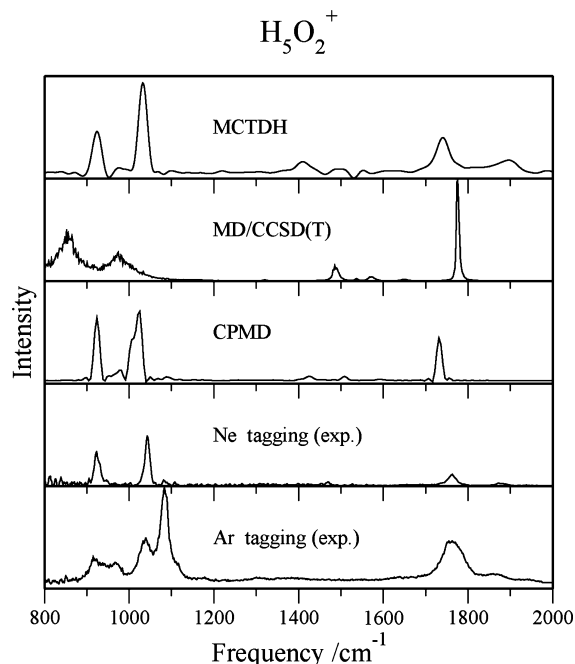


Figure 3. Comparison of the H_5O_2^+ MD/CCSD(T), CPMD, and MCTDH (0 K)^{17,40} simulations of the IR spectrum and $\text{H}_5\text{O}_2^+\text{RG}$ (RG = Ar, Ne) experimental observations.^{14,38,39}

calculations with the BLYP functional giving too high a value for the harmonic frequency of the shared proton stretch.

The relative intensities and widths of the two features comprising the shared proton doublet are different in the two MD approaches. For example, for the $T = 30\text{ K}$ simulations, the two peaks are of comparable intensity in the CPMD simulations, whereas the lower energy peak is about twice as intense as the higher energy peak in the simulations using the CCSD(T) PES. At $T = 50\text{ K}$ the two peaks are of comparable intensity in the MD/CCSD(T) simulation but differ by over an order of magnitude in intensity in the CPMD simulations. We note further that the doublet in the region of the shared proton stretch is still discernible in the spectrum obtained from the MD/CCSD(T) simulations at $T = 100\text{ K}$ and reported in ref 16. The differences in the widths are most likely due to the fact that the CPMD calculations are microcanonical whereas the MD/CCSD(T) calculations are canonical; however, differences in the electronic description of the H^+ coupling could also contribute.

In spite of the shortcomings, discussed above, the success of the MD simulations at recovering the shared proton doublet is most encouraging, as is the overall good agreement between the results of the two MD approaches since the CPMD method can be applied to much larger clusters than can MD simulations on high-quality predetermined ab initio potentials. In the remainder of the paper, we focus on the results obtained from the $T = 30\text{ K}$ simulations, although, on the basis of the MD/CCSD(T) results for H_5O_2^+ , it is possible that the inert gas atom tagged clusters studied experimentally are somewhat warmer than this.

B. Comparison of Measured and Calculated Spectra. In addition to $\text{H}_5\text{O}_2^+\text{Ne}$ and $\text{H}_5\text{O}_2^+\text{Ar}$, experimental predissociation spectra have also been reported for the Ar tagged complexes of D_5O_2^+ , D_4HO_2^+ , and DH_4O_2^+ (in this case only in the spectral region above 2200 cm^{-1}).^{38,39} In the latter two cases, multiple isomers are possible as the minority species (H or D) can be located in the shared position between the O atoms or in one of the free hydroxy sites and, in addition, the Ar atom can bind

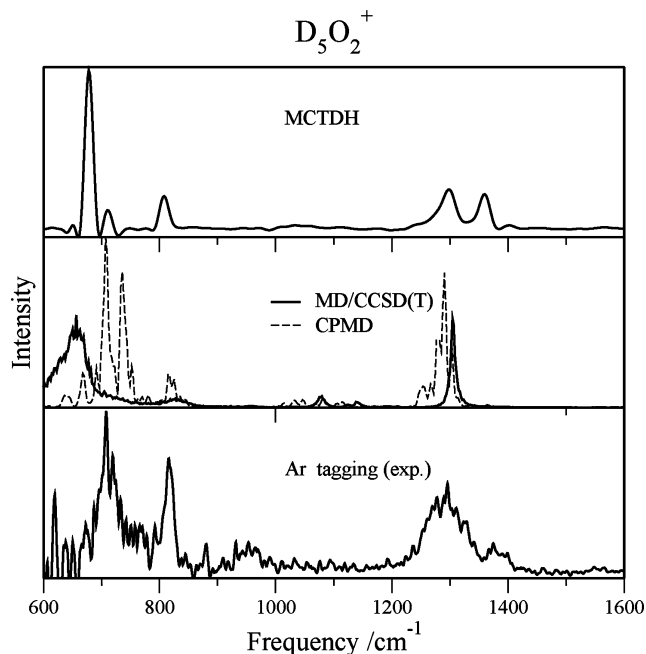


Figure 4. Computed IR spectra of $D_5O_2^+$ at the MD/CCSD(T) and CPMD levels of theory with corresponding MCTDH (0 K) spectra⁴⁰ and Ar predissociation spectra.³⁸

to any of the free OH (OD) groups. Earlier theoretical analyses^{23,38} have shown that, due to zero-point energy (ZPE) differences, the energetically favored isomers are $D_4HO_2^+(int)$ and $DH_4O_2^+(ext)$, where the “int” and “ext” labels indicate the isomers with the minority species (H or D) located in the shared proton position and as a free OD (OH), respectively. In other words, in the mixed isotopologues, the vibrational zero-point energy contributions favor locating a H atom in the shared proton site.

i. Free OH (OD) Stretch Region of the Spectra. The experimental vibrational predissociation spectrum of $H_5O_2^+Ne$ has two strong transitions split by about 100 cm^{-1} in the free OH region. In agreement with experiment, both the $T = 30\text{ K}$ CPMD and MD/CCSD(T) simulations and the harmonic frequency calculations on $H_5O_2^+$ give two transitions, split by about 100 cm^{-1} , due to the asymmetric and symmetric stretch modes of the water molecules. These results indicate that the Ne atom does not significantly perturb the $H_5O_2^+$ ion core. On the other hand, the predissociation spectrum of $H_5O_2^+Ar$ differs significantly from that of $H_5O_2^+Ne$ in the free OH stretch region of the spectrum. This is a consequence of the “strong” binding of the Ar atom to one of the H atoms, leading to a sizable red shift of the associated stretch vibration. The influence of the Ar atom on the free OH (OD) spectra of $H_5O_2^+$ and its D-substituted isotopologues is well accounted for by harmonic frequency calculations on the Ar tagged ions.¹⁴ For this reason, in the ensuing discussion of the vibrational spectra of $H_5O_2^+$ and its D-substituted isotopologues, we focus on the more challenging lower frequency region.

ii. Bending Region of the Spectra. Figures 3–5 report the low-frequency spectra of $H_5O_2^+$, $D_5O_2^+$, $D_4HO_2^+$, and $DH_4O_2^+$ obtained from $T = 30\text{ K}$ MD/CCSD(T) and CPMD simulations, 0 K MCTDH calculations,^{17,18,40} and Ar-atom predissociation measurements.^{14,38,39} Figure 6 shows calculated spectra for $DH_4O_2^+$. For $H_5O_2^+$, Figure 3 also includes the Ne atom predissociation spectrum.¹⁴ For $DH_4O_2^+$ and $D_4HO_2^+$, MD results are reported for both the “exterior” and “interior” isomers, while MCTDH results are available only for the interior isomers.

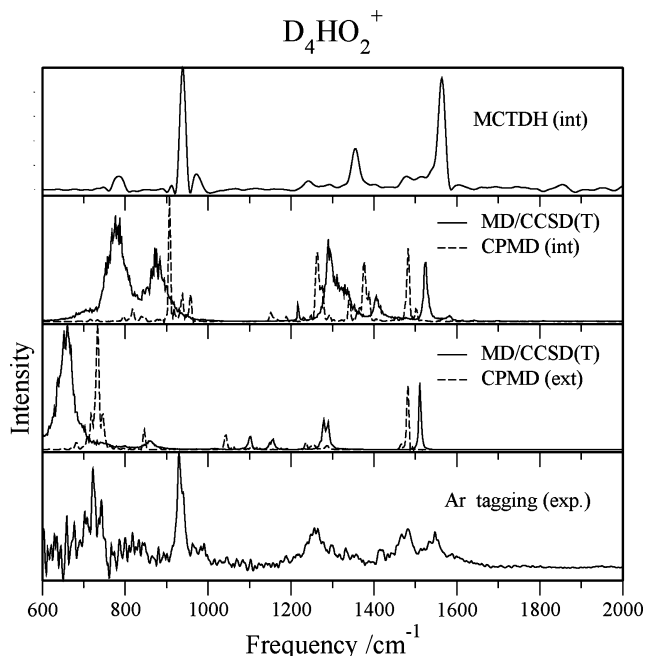


Figure 5. IR spectra of mixed H/D isotopologues $D_4HO_2^+$ calculated using the MD/CCSD(T) and CPMD methods with hydrogen in both interior and exterior positions. The corresponding MCTDH (0 K) spectra⁴⁰ are shown only for the interior isomer. The presented experimental spectra are for $D_4HO_2^+Ar$.

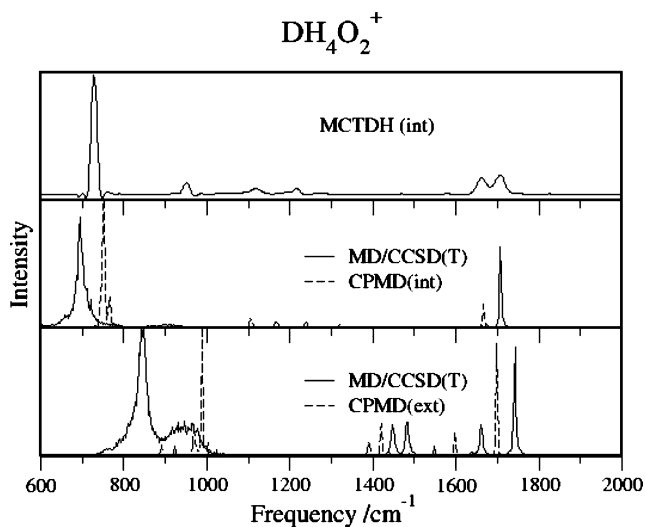


Figure 6. IR spectra of mixed H/D isotopologues $DH_4O_2^+$ calculated using the MD/CCSD(T) and CPMD methods with deuterium in both interior and exterior positions. MCTDH simulations (0 K)⁴⁰ are shown only for the interior isomer.

For each isotopologue the spectra obtained using the two MD approaches are in fairly good agreement, and for that reason, we focus on the results obtained using the MD/CCSD(T) approach.

The vibrational predissociation spectra of all isotopologues considered display more structure in the bending regions than would be expected on the basis of the harmonic frequency calculations. Specifically, the predissociation spectra of $H_5O_2^+Ne$, $H_5O_2^+Ar$, and $D_5O_2^+Ar$ each display two peaks in the bending regions, and that of $D_4HO_2^+Ar$ displays background structure throughout the $1170\text{--}1650\text{ cm}^{-1}$ range, with three peaks superimposed on the broad structure. As will be discussed below, we believe the additional bands in the spectra arise from Fermi resonances and possibly also the presence of both interior

and exterior isomers in the case of DH_4O_2^+ and D_4HO_2^+ . Indeed, McCunn et al. presented evidence that both isomers contribute to their experimental Ar-tagged spectra.^{38,39}

For H_5O_2^+ and D_5O_2^+ the experimental predissociation spectra display broad bands centered near 1760 and 1300 cm^{-1} , respectively, with weak shoulders about 100 cm^{-1} to the blue of the intense features. The MD/CCSD(T) simulations on H_5O_2^+ and D_5O_2^+ give strong transitions near 1780 and 1300 cm^{-1} , respectively, very close to the corresponding harmonic frequencies for the bending vibrations reported in Table 1. We conclude, therefore, as did Meyer and co-workers on the basis of analysis of the results of their MCTDH calculations, that the strong transitions near 1760 and 1300 cm^{-1} are due to the HOH and DOD bending vibrations, respectively. Interestingly, the weak satellite bands that show up in the measured spectra $\sim 110 \text{ cm}^{-1}$ to the blue of the bending transitions and which are absent in the MD spectra are recovered in the MCTDH calculations. This appears to be a shortcoming of the MD calculations. In the case of H_5O_2^+ , Meyer and co-workers assigned the satellite band to a combination state dominated by one quantum in the shared proton stretch and two quanta in the water–water stretch. The peak to the blue of the bending transition of D_5O_2^+ was not assigned by Meyer and co-workers, although they did note that it does not correspond to a combination band involving shared proton stretch and water–water stretch.

The measured predissociation spectrum of D_4HO_2^+ displays moderately strong bands near 1260, 1480, and 1520 cm^{-1} and a weak feature near 1400 cm^{-1} . The MD/CCSD(T) simulations on the more stable $\text{HD}_4\text{O}_2^+(\text{int})$ isomer give six features in the bending region (strong features at 1300 and 1525 cm^{-1} , medium-strength transitions at 1400 and 1330 cm^{-1} , and very weak transitions at 1230 and 1580 cm^{-1}). The 1230, 1300, 1525, and 1580 cm^{-1} features in the MD/CCSD(T) spectra fall close to the harmonic frequencies for the bend and shared proton perpendicular vibrations. On this basis, we conclude that the 1230 and 1300 cm^{-1} transitions from the MD/CCSD(T) simulations are due to the DOD bending vibrations and that the two higher energy transitions are due to the perpendicular motion of the shared proton. The MCTDH calculations on $\text{D}_4\text{HO}_2^+(\text{int})$ give two strong transitions near 1355 and 1560 cm^{-1} , with the former being due to a bending mode and the latter to a combination band involving one quantum of the shared proton stretch and one quantum of the water–water stretch. The MCTDH calculations also give several weak unassigned features in the 1200–1550 cm^{-1} range.

The calculated spectra for DH_4O_2^+ in Figure 6 show significant differences for the interior and exterior isomers. The MD/CCSD(T) and CPMD simulations of the higher energy $\text{DH}_4\text{O}_2^+(\text{int})$ isomer give a single strong transition near 1710 cm^{-1} , close to the 1740 cm^{-1} HOH bending frequency found in the harmonic calculations. The MCTDH calculations on $\text{DH}_4\text{O}_2^+(\text{int})$ predict a doublet of roughly equal intensity peaks near 1660 and 1720 cm^{-1} . The 1660 cm^{-1} feature in the MCTDH spectrum is associated with the water bend, and the 1720 cm^{-1} feature with a combination band involving one quantum of the shared D^+ stretch plus two quanta of the water–water stretch. This doublet is not captured by the classical simulations. The MD/CCSD(T) and CPMD calculations for the lower energy $\text{DH}_4\text{O}_2^+(\text{ext})$ isomer display intense features near 1700 cm^{-1} , with a number of satellite features between 1400 and 1650 cm^{-1} ; these are in rough accord with the harmonic frequencies of this isomer. (MCTDH calculations were not reported for this isomer.) If both isomers play a role in the Ar tagging experiment, as suggested by experimental results

published in the OH/OD stretch regions of the spectrum,³⁹ then the present calculations suggest a rather complex spectrum in this region.

iii. O–H–O (O–D–O) Asymmetric Stretch Region of the Spectra. We now turn our attention to the vibrational spectra in the shared proton stretch region. As noted in the Introduction, the experimental predissociation spectrum of $\text{H}_5\text{O}_2^+\text{Ne}^{14}$ (Figure 3) displays a doublet (peaks at 928 and 1047 cm^{-1}) in the shared proton stretch region. In going from $\text{H}_5\text{O}_2^+\text{Ne}$ to $\text{H}_5\text{O}_2^+\text{Ar}$ each member of the doublet in the former is “split” into a pair of doublets. Since none of the calculations (discussed below) on the bare ion show this pair of doublets, we conclude that they are induced by the Ar atom, rather than being intrinsic to H_5O_2^+ . The Ar atom interacts much more strongly with the H_5O_2^+ ion than does the Ne atom (as is apparent from the spectra in the free OH stretch region), and since the inert gas atom preferentially binds to one of the dangling H atoms, this results in a greater degree of symmetry breaking in the Ar case.^{14,22} Thus, we speculate that the extra structure in the shared proton asymmetric stretch region of the spectrum of $\text{H}_5\text{O}_2^+\text{Ar}$ is a consequence of the mixing with what would otherwise be dark overtone states involving the water–water stretch and water wag.

Both the MD/CCSD(T) and MCTDH calculations on H_5O_2^+ give two strong features in the region of the shared proton stretch, with energies of 850 and 980 cm^{-1} and 910 and 1025 cm^{-1} , respectively, in good agreement with the experimental results for $\text{H}_5\text{O}_2^+\text{Ne}$. As noted above, the underestimation of the energies of the features from the MD simulations could be the result of an incomplete recovery of the anharmonicity of the potential energy surface. The 850 cm^{-1} band found in the MD/CCSD(T) simulations falls very close to the harmonic frequency for the shared proton stretch, which suggests that the lower energy component of the MD doublet is likely to be dominated by shared proton stretch motion. Indeed, this is confirmed by the driven MD simulations of Kaledin et al.¹⁶ On the other hand, the lower energy component of the doublet in the MCTDH calculations derives primarily from a combination state involving one quantum of the water–water stretch and two quanta of the water wag, while the higher energy member of the doublet is dominated by the shared proton stretch. For such strongly perturbed states, these differences between the assignments based on classical and quantum calculations are not surprising.

Consider next the spectra of D_5O_2^+ shown in Figure 4. The vibrational predissociation spectrum of $\text{D}_5\text{O}_2^+\text{Ar}$ displays intense features near 705 and 810 cm^{-1} , which are about 250 cm^{-1} to the red of the corresponding doublet in the predissociation spectrum of $\text{H}_5\text{O}_2^+\text{Ne}$. The doublet structure in the region of the shared proton stretch is recovered by the MD/CCSD(T) and MCTDH calculations, with bands near 650 and 830 cm^{-1} in the former and near 680 and 805 cm^{-1} in the latter. The 650 cm^{-1} band in the MD/CCSD(T) spectrum is close to the harmonic frequency (Table 1). In the MCTDH calculations, the lower energy band has as its dominant component the shared proton stretch and the higher energy band is primarily due to the combination state, comprised of one quantum of the water–water stretch and two quanta of the wag. Both sets of calculations predict the lower energy band to be much more intense than the higher energy band, whereas the difference in intensity is only about 1.5:1 in the experimental spectrum. This difference in the relative intensities in the calculated and measured spectra of the higher energy peak in the measured

spectrum is likely due to the presence of the Ar atom in the experimentally probed ions.

In the case of $D_4HO_2^+Ar$, the experimental spectrum, shown in Figure 5, displays in the shared proton stretch region two strong bands of nearly equal intensity at 720 and 930 cm^{-1} as well as a weak feature near 800 cm^{-1} . On the basis of simple considerations, the 720 cm^{-1} band might be expected to be due to the exterior (H in the exterior) and the 930 cm^{-1} band to the interior (H on the interior) isomer. For $D_4HO_2^+(int)$ the MD/CCSD(T) calculations give a doublet at 775 and 885 cm^{-1} , slightly to the red of the doublet calculated for $H_5O_2^+$, and in good accord with experiment. The MCTDH calculations on $D_4HO_2^+(int)$ give a strong peak at 930 cm^{-1} in excellent agreement with experiment, but the feature near 775 cm^{-1} does not correspond as well with the experimental feature at 720 cm^{-1} . Analysis of the MCTDH wave functions shows that the intense peak has as its major component the shared proton stretch, and that the weak 775 cm^{-1} feature is due to a combination band involving one quantum of the water–water stretch and two quanta of the wag. The MD/CCSD(T) simulations on the exterior isomer give a single intense line at 660 cm^{-1} , close to that calculated for $D_5O_2^+$. This intense feature is not seen in the calculated spectra of $D_4HO_2^+(int)$; however, it may correspond to the spectral congestion seen in the region between 600 and 700 cm^{-1} . Comparison of the calculated and experimental spectra is clearly complicated by the possible presence of both isomers and perturbation of the associated spectra by the Ar atom, as noted by McCunn et al.^{38,39}

Finally, we consider the calculated spectra of $DH_4O_2^+$, shown in Figure 6. The spectrum of $DH_4O_2^+(int)$ for both the MD/CCSD(T) and MCTDH calculations gives a single intense transition near 700 cm^{-1} , at essentially the same location as for the shared proton stretch in the harmonic calculations. The MD/CCSD(T) spectrum for the lower energy $DH_4O_2^+(ext)$ shows a doublet feature that is blue-shifted relative to the intense peak for $DH_4O_2^+(int)$. This feature is not found in the CPMD spectrum, and thus, it will be interesting for future experiments and perhaps new MCTDH calculations for $DH_4O_2^+(ext)$ to explore this region of the spectrum.

IV. Conclusions

The present investigation shows that classical MD simulations at a temperature of 30 K qualitatively reproduce many of the key features in the experimental vibrational predissociation spectra of $H_5O_2^+$ and its D-substituted isotopologues. Most strikingly, the MD simulations give Fermi resonance doublets in the region of the shared proton stretch of $H_5O_2^+$, $D_5O_2^+$, $D_4HO_2^+$, and $DH_4O_2^+$. In the latter two cases, the more stable isomer, i.e., the one with H^+ “in the middle”, appears to dominate the experimental spectrum; it is clear from both experiment and the present calculations that the less stable isomer is present in the experimental spectra. Without a quantitative measure of the relative contributions of the two isomers, it is difficult to make a quantitative comparison between the experimental and calculated spectra. A further complication in comparing the calculated and measured spectra of $H_5O_2^+$ and its isotopologues is that the calculations have been performed for the bare ions, and the experimental spectra have been obtained by predissociation of attached inert gas atoms. Only for $H_5O_2^+$ are experimental results available for a Ne atom tag. For the other isotopologues the vibrational predissociation spectra have been measured with the more strongly perturbing Ar atom tag.

Overall the spectra obtained from the CPMD simulations using the BLYP density functional method are similar to those

obtained from the MD simulations using the CCSD(T) potential energy surface, which is encouraging as AIMD simulations using DFT functionals are applicable to much larger clusters. Comparison of the spectra from the MD simulations to those from the MCTDH calculations does show several significant differences, particularly with regard to the relative intensities of some of the bands. These differences appear to be due primarily to the low-temperature MD simulations underestimating diagonal anharmonicities which are especially important for the shared proton stretch and wag vibrations of $H_5O_2^+$ and its isotopologues.

Acknowledgment. J.M.B. and K.D.J. thank the National Science Foundation (NSF Grants CHE-0446527 and CHE-518253) for funding this project. M.K. thanks the Research Corp. (Cottrell College Science Award No. 7725) for support of this work. We thank Mark Johnson and Hans-Dieter Meyer for sending digital versions of their spectra.

References and Notes

- (1) Atkins, P. W. *Physical Chemistry*, 7th ed.; Freeman: New York, 2002.
- (2) Zundel, G. In *The Hydrogen Bond: Recent Developments in Theory and Experiment*; Schuster, P., Zundel, G., Sandorfy, C., Eds.; North-Holland: Amsterdam, 1976; Vol. II, p 683.
- (3) Giruere, P. A.; Turrel, S. *Can. J. Chem.* **1976**, *54*, 3477.
- (4) Librovich, N. B.; Sakun, V. P.; Sokolov, N. D. *Chem. Phys.* **1979**, *39*, 351.
- (5) Eigen, M.; Wicke, E. *J. Phys. Chem.* **1954**, *58*, 702.
- (6) Zundel, G.; Metzger, H. *Z. Phys. Chem. (Muenchen, Ger.)* **1968**, *58*, 225.
- (7) Agmon, N. *Chem. Phys. Lett.* **1995**, *244*, 456.
- (8) Yeh, L. I.; Okumura, M.; Myers, J. D.; Price, J. M.; Lee, Y. T. *J. Chem. Phys.* **1989**, *91*, 7319.
- (9) Asmis, K. R.; Pivonka, N. L.; Santambrogio, G.; Brummer, M.; Kaposta, C.; Neumark, D. M.; Woste, L. *Science* **2003**, *299*, 1375.
- (10) Fridgen, T. D.; McMahon, T. B.; MacAleese, L.; Lemaire, J.; Maitre, P. *J. Phys. Chem. A* **2004**, *108*, 9008.
- (11) Headrick, J. M.; Bopp, J. C.; Johnson, M. A. *J. Chem. Phys.* **2004**, *121*, 11523.
- (12) Jiang, J.-C.; Wang, Y.-S.; Chang, H.-C.; Lin, S. H.; Lee, Y. T.; Niedner-Schatteburg, G.; Chang, H.-C. *J. Am. Chem. Soc.* **2000**, *122*, 1398.
- (13) Headrick, J. M.; Diken, E. G.; Walters, R. S.; Hammer, N. I.; Christie, R. A.; Cui, J.; Myshakin, E. M.; Duncan, M. A.; Johnson, M. A.; Jordan, K. D. *Science* **2005**, *308*, 1765.
- (14) Hammer, N. I.; Diken, E. G.; Roscioli, J. R.; Johnson, M. A.; Myshakin, E. M.; Jordan, K. D.; McCoy, A. B.; Bowman, J. M.; Carter, S. *J. Chem. Phys.* **2005**, *122*, 244301.
- (15) McCunn, L.; Roscioli, J. R.; Johnson, M. A.; McCoy, A. B. *J. Phys. Chem. B* **2008**, *112*, 321.
- (16) Kaledin, M.; Kaledin, A. L.; Bowman, J. M. *J. Phys. Chem. A* **2006**, *110*, 2933.
- (17) Vendrell, O.; Gatti, F.; Meyer, H.-D. *Angew. Chem., Int. Ed.* **2007**, *46*, 6918.
- (18) Vendrell, O.; Gatti, F.; Meyer, H.-D. *J. Chem. Phys.* **2007**, *127*, 184303.
- (19) Beck, M. H.; Jackle, A.; Worth, G. A.; Meyer, H.-D. *Phys. Rep.* **2000**, *234*, 1.
- (20) Huang, X.; Braams, B. J.; Bowman, J. M. *J. Chem. Phys.* **2005**, *122*, 044308.
- (21) Sauer, J.; Dobler, J. *ChemPhysChem* **2005**, *6*, 1706.
- (22) Park, M.; Shin, I.; Singh, N. J.; Kim, K. S. *J. Phys. Chem. A* **2007**, *111*, 10692.
- (23) Devlin, J. P.; Severson, M. W.; Mohamed, F.; Sadlej, J.; Buch, V.; Parrinello, M. *Chem. Phys. Lett.* **2005**, *408*, 439.
- (24) Car, R.; Parrinello, M. *Phys. Rev. Lett.* **1985**, *55*, 2471.
- (25) Marx, D.; Hutter, J. In *Modern Methods and Algorithms of Quantum Chemistry*; Grotendorst, J., Ed.; NIC; FZ Jülich: Jülich, Germany, 2000; pp 301–449.
- (26) Becke, A. D. *Phys. Rev. A* **1988**, *38*, 3098.
- (27) Lee, C.; Yang, W.; Parr, R. C. *Phys. Rev. B* **1988**, *37*, 785.
- (28) Troullier, N.; Martins, J. L. *Phys. Rev. B* **1991**, *110*, 2810.
- (29) Martyna, J.; Tuckerman, M. E. *J. Chem. Phys.* **1999**, *110*, 2810.
- (30) Nosé, S. *Mol. Phys.* **1984**, *52*, 255.
- (31) Nosé, S. *J. Chem. Phys.* **1984**, *81*, 511.
- (32) Hoover, W. G. *Phys. Rev. A* **1985**, *31*, 1695.
- (33) Kumar, P. P.; Marx, D. *Phys. Chem. Chem. Phys.* **2006**, *8*, 573.

(34) Kuo, I.-F. W.; Mundy, C. J.; McGrath, M. J.; Siepmann, J. I. *J. Chem. Theory Comput.* **2006**, 2, 1274.

(35) Ramirez, R.; López-Ciudad, T.; Kumar, P. P.; Marx, D. *J. Chem. Phys.* **2004**, 121, 3973.

(36) Berens, P. H.; Wilson, K. R. *J. Chem. Phys.* **1981**, 74, 4872.

(37) Hutter, J.; et al. CPMD. <http://www.cpmc.org/>. Copyright IBM Corp. 1990–2006. Copyright MPI für Festkörperforschung Stuttgart 1997–2001.

(38) McCunn, L. R.; Roscioli, J. R.; Johnson, M. A.; McCoy, A. B. *J. Phys. Chem. B* **2008**, 112, 321.

(39) McCunn, L. R.; Roscioli, J. R.; Elliott, B. M.; Johnson, M. A.; McCoy, A. B. *J. Phys. Chem. A* **2008**, 112, 6074.

(40) Vendrell, O.; Gatti, F.; Meyer, H.-D. *Angew. Chem., Int. Ed.* **2009**, 48, 352.

JP900737R